Structure, Microstructure and Hyperfine Interactions in Hf- and Ni-Substituted TiFe Alloy for Hydrogen Storage

K. Komędera[a,b,*], J.M. Michalik[a], K. Sworst[a] and Ł. Gondek[a]

[a] *AGH University of Krakow, Faculty of Physics and Applied Computer Science, Department of Solid State Physics, Mickiewicza 30, 30-059 Kraków, Poland*
[b] *University of the National Education Commission, Mössbauer Spectroscopy Laboratory, Podchorążych 2, 30-084 Kraków, Poland*

Doi: 10.12693/APhysPolA.146.215 *e-mail: komedera@agh.edu.pl

Hydrogen storage in metallic materials is of utmost importance for hydrogen energy applications. In this paper, we address the issue of finding cost-effective materials for large-scale usage. One such material is TiFe, which requires high H_2 pressure and temperature above 400°C to activate and start reversibly absorbing/desorbing hydrogen. To facilitate the aforementioned processes, the alloy must be subjected to doping by other elements. We report research on the $Ti_{1-x}Hf_xFe_{1-y}Ni_y$ compounds and their hydrides investigated by means of X-ray diffraction, electron microscopy, and Mössbauer spectroscopy. The data show that for $Ti_{0.9}Hf_{0.1}Fe_{0.9}Ni_{0.1}$, the activation temperature is reduced to 200°C, with a slightly reduced total hydrogen absorption. According to Mössbauer spectroscopy results, hydrogenation of the synthesized alloys leads to a significant decrease in the electronic state of the compounds, as could be expected for hydrides. It also proves the existence of structural disorder introduced to facilitate the activation of the alloys, complementary to X-ray diffraction and electron microscopy.

topics: hydrogen storage, FeTi alloys, Mössbauer spectroscopy, X-ray diffraction

1. Introduction

Transformation of the industry with regard to low emission of greenhouse gases requires a complex approach to energy production, storage, and usage. In this context, hydrogen energy is recognized as a crucial part of the transformation. However, a wide introduction of hydrogen as an energy carrier requires the rapid development of sustainable technologies for hydrogen production, purification, storage, and conversion into electric power. For the above-mentioned applications, metal-hydrides are developed, however, most of the alloys contain rare earths, noble metals, or other expensive elements (e.g., $LaNi_5$).

Therefore, a lot of research is done on intermetallic hydrides in AB5, AB2, and AB systems. The latter, based on TiFe composition, are considered the most cost-effective [1–4], since the alloys can be produced even from low-cost recycled steels and alloys [1]. Although TiFe-based alloys surpass the commonly used $LaNi_5$ derivatives, reaching a gravimetric concentration of hydrogen above 1.6 wt.%, their activation and durability are crucial issues [1–3]. As Ti and Fe exhibit high affinity towards oxidation, the TiFe-based alloys are known to have demanding activation procedures for hydrogen absorption. If the initial powders were exposed to air, their activation requires high H_2 pressures, typically above 60 bar, and high-temperature treatment (above 400°C) [4, 5]. As can be seen, the first reports on the nature of grain surface passivation involving the formation of oxides/hydroxides date back to the 80s of the last century [5]. Surprisingly, the studies were not extensively continued as the AB5 alloys offered much better stability and ease of the activation procedure [5]. Due to the large-scale need for hydrogen-absorbing alloys for hydrogen energy applications, it turned out that the availability of constituting elements, providing low-cost material, is crucial for the development of metal hydrides [1]. For this reason, TiFe alloys are nowadays highly researched materials, as the cost of 1 kg of alloy is around 15 USD when made of pure elements and as low as 2–3 USD when Ti and Fe are obtained from recycled materials [1, 3], while prices of the commercially used $LaNi_5$ derivatives range between 80 and 100 USD per 1 kg.

For these reasons, research on facilitating the activation and durability of TiFe alloys for hydrogen storage is of high importance. Even incorporating small amounts of precious materials into TiFe alloys is economically reasonable. Indeed, one of the ways to achieve the goal is by introducing elements such as Mn, Cr, Ni, Co, Nb, Zr, or Mm, where Mm

stands for mischmetal (a mixture of light rare-earth metals, mainly Ce, La, and Nd) [6–11]. It is well established that substituting Ni for Fe facilitates activation and lowers the equilibrium pressure required to hydrate the alloy [2, 11]. Also, the introduction of Zr for Ti offers similar effects, however, the total gravimetric density of hydrogen decreases because Zr is a 4d metal [2]. Also, 5d elements such as Hf were considered as dopants for TiFe alloys [4, 12]. It was shown that, while the overall gravimetric density of hydrogen is decreased (for the same reason as for Zr substitutions), the activation is much easier and does not require high temperatures. However, cycling stability is reduced as the addition of Hf results in additional Hf-rich hexagonal Laves phases and cubic incursions of Ti-rich grains [12].

In our work, we focus our research on finding a way to reduce the possibility of the appearance of additional phases by implementing the Hf and Ni into the TiFe matrix as substituting elements to form $Ti_{1-x}Hf_xFe_{1-y}Ni_y$ alloys. The research involves (i) microstructural and structural studies by X-ray diffraction (XRD) and scanning electron microscopy with X-ray microprobe analysis (scanning electron microscopy (SEM) + energy-dispersive X-ray spectroscopy (EDS)), (ii) sorption measurements made by means of volumetric Sieverts' setup, and (iii) hyperfine interactions of Fe atoms observed by Mössbauer spectroscopy.

2. Experimental procedures and hydride synthesis

The $Ti_{1-x}Hf_xFe_{1-y}Ni_y$ alloys were synthesized by arc melting of stoichiometric amounts of elements of 99.9% purity in a high-purity Ar (6 N) atmosphere with Zr as a getter. The resulting buttons of a mass of about 2 g were remelted several times to achieve homogeneity. After synthesis, the alloys were not subjected to the usual annealing in order to keep a certain degree of atomic disorder, which facilitates the appearance of surface segregation, related mainly to magnetic 3d metals under a hydrogen atmosphere. Surface segregation hampers the appearance of the oxide passivation layer at grain boundaries, resulting in easier access of H_2 molecules to the metallic interface. On the other hand, the appearance of strains and static defects in the structure is favorable for providing life-cycle stability, which is essential for future applications.

The samples were hydrided using the Setaram PCTPro volumetric sorption analyzer. For activation, the first hydrogen uptake, the powdered sample of known mass (approximately 0.2 g), was placed in an Inconel steel container connected to calibrated volumes and pressure transducers. The dead volume of the sample container was calculated by expanding He (6 N) from the known volume into the container. Then, the calibrated volume was filled with hydrogen (6 N) at a pressure of 100 bar. After exposing the sample to hydrogen, the pressure was about 65 bar, and the container was slowly heated to 400°C (5°C/min) to track the temperature at which the hydrogen uptake occurred. Then, the sample was cooled to that temperature and kept at it for 12 h. Afterward, the sample was slowly cooled to room temperature to precisely estimate the amount of absorbed hydrogen.

TABLE I

Results of hydrogenation in the obtained samples.

Sample	Final hydrogen concentration [wt.%]	Absorption onset during activation[°C]
TiFe	1.62(1)	285
$Ti_{0.8}Hf_{0.2}Fe$	–	–
$Ti_{0.9}Hf_{0.1}Fe_{0.9}Ni_{0.1}$	1.43(2)	200
$Ti_{0.8}Hf_{0.2}Fe_{0.8}Ni_{0.2}$	1.24(3)	225

As can be seen in Table I, the parent TiFe alloy was hydrided for the first time (activated) at a relatively low temperature, compared to the temperatures reported in the literature [2, 4, 5, 11]. It was impossible to hydride the $Ti_{0.8}Hf_{0.2}Fe$ alloy using the same procedure. Interestingly, for Hf added as a catalyst (without substitution of the constituents of the alloy) to the TiFe alloy, the absorption of hydrogen was reported as marginal [12]. There is a consensus in the literature regarding the positive influence of Ni on the pressure for charging the Ni-doped alloys as well as on the activation temperatures. The data revealed that both parameters decrease with Ni content. However, there are mixed reports on the systematics of these effects with Ni concentration [4, 11, 13]. For example, $TiFe_{1-x}Ni_x$ alloys can be activated at 300°C ($x = 0.0$ and $x = 0.1$), 250°C ($x = 0.2$), and 170°C ($x = 0.4$) [13]. As evident from Table I, the structural disorder substantially facilitates the activation of the alloys, confirming the surface segregation in as-cast materials. The obtained materials are stable in the ambient condition, while the hydrogen can be easily desorbed at temperatures above 50°C.

Then, the parent samples and their hydride structure, microstructure, and composition were examined by XRD and SEM using an Empyrean powder diffractometer equipped with a copper tube (Cu K_α) and JEOL 5900 LV electron microscope. The diffraction patterns were refined by Rietveld-type FullProf Suite [14] with LaB_6 sample (NIST660) used as a calibration of the line profiles and positions. Mössbauer spectra have been collected in standard transmission geometry for 14.4 keV transition in ^{57}Fe by using a commercial $^{57}Co(Rh)$ source kept under ambient pressure and at room temperature. The absorber was made in

TABLE II

Structural parameters of the cubic Pm-3m phase derived from Rietveld refinements.

Sample	Lattice param. [Å]	Strain [%]	Contribution [%]
TiFe	2.9773(2)	0.42(1)	100
$Ti_{0.8}Hf_{0.2}Fe$	2.9930(8)	0.93(4)	59(3)
$Ti_{0.9}Hf_{0.1}Fe_{0.9}Ni_{0.1}$	2.9889(2)	0.65(3)	76(1)
$Ti_{0.8}Hf_{0.2}Fe_{0.8}Ni_{0.2}$	3.0139(2)	0.61(2)	80(2)

powder form by mixing 25 mg of the alloy with the BN carrier. The absorber thickness then amounted to 18.85 mg/cm^2. Spectral shifts are reported in relation to ambient pressure and room temperature natural α-Fe. Spectra were fitted within transmission integral approximation by means of PMOS software.

3. Results and discussion

The stoichiometric TiFe alloy crystallizes in the cubic system, adopting the Pm-3m space group [4]. In this primitive unit cell, the Ti atoms occupy the 1b site $(1/2; 1/2; 1/2)$, and the Fe atoms are placed in the 1a site $(0; 0; 0)$. For non-stoichiometric alloys, an additional phase doped with Zr or Hf, namely the hexagonal Laves (C14) phase, was evidenced [4].

X-ray diffraction patterns of prepared alloys are presented in Fig. 1. All diffraction patterns were refined to track changes in the parameters of the primary cubic phase. The obtained parameters are listed in Table II. For the TiFe alloy, the pattern can be indexed entirely and refined with the cubic Pm-3m space group. No additional reflections were observed. Rietveld refinement revealed some mixing of the Ti and Fe atoms between the 1b and 1a sites. Up to 15% of the Ti atoms were found in the Fe lattice (on the 1a site), while the same amount of Fe atoms was distributed over the 1b site. The reflections are relatively broad, showing a significant amount of strain, which apparently originated from atomic disorder. As mentioned in the experimental section, this effect was expected to have a positive influence on the hydriding properties of the alloys. For $Ti_{0.8}Hf_{0.2}Fe$, the pattern clearly shows two sets of reflections, the main cubic Pm-3m one and the additional hexagonal $P6_3/mmc$ phase (C14 Laves phase). However, the reflections are very broad, which most likely corresponds to the distribution of composition in both structures. For the $Ti_{0.9}Hf_{0.1}Fe_{0.9}Ni_{0.1}$ sample, the C14 phase is suppressed compared to purely Hf-substituted alloy, as apparent from Fig. 1 and Table II. Similarly, the $Ti_{0.8}Hf_{0.2}Fe_{0.8}Ni_{0.2}$ alloy exhibits about 80% of the cubic phase.

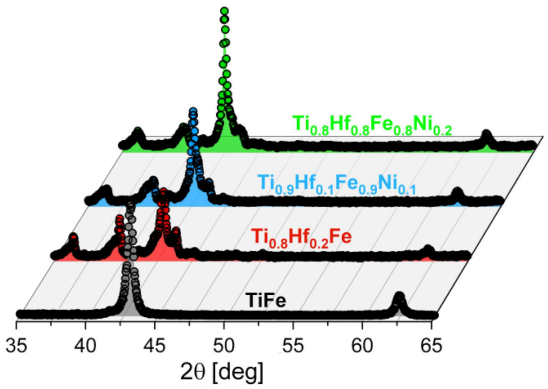

Fig. 1. X-ray diffraction patterns of synthesized $Ti_{1-x}Hf_xFe_{1-y}Ni_y$ alloys.

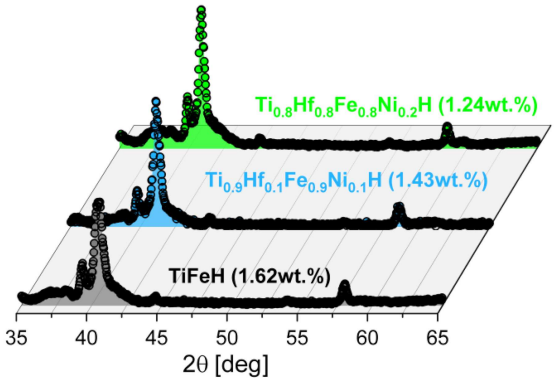

Fig. 2. X-ray diffraction patterns of obtained hydrides.

As is apparent from Table II, the lattice parameters are larger after introducing Hf into the alloy, as Hf possesses a larger metallic radius than Ti, and this, along with the fact that the metallic radius of Ni is marginally smaller than that of Fe, leads to observed expansion of the cubic lattice. Interestingly, the $Ti_{0.8}Hf_{0.2}Fe$ lattice parameter for the cubic phase is smaller than that for $Ti_{0.8}Hf_{0.2}Fe_{0.8}Ni_{0.2}$. This is related to the precipitation of the Hf-rich phase in the former alloy. Therefore, the Hf content in the cubic phase is less than would be expected from stoichiometry. In contradiction, the simultaneous substitution of Ni stabilizes the cubic phase; hence, more Hf is incorporated into the cubic structure. Analysis of the strains, which reflects the level of static defects present in the structure, suggests that the cubic structure in the $Ti_{0.8}Hf_{0.2}Fe$ alloy is heavily affected by defects originating from non-stoichiometry. The strains in the primary cubic structure for double-substituted TiFe alloys are significantly smaller, yet still above the level of the pure TiFe compound. The refinements revealed that the best reliability factors were found where the hafnium atoms substituted the Ti (1b) site, while the Ni atoms were placed in the Fe (1a) site exclusively. It can be concluded that

TABLE III

Structural parameters of the orthorhombic $P222_1$ phase derived from Rietveld refinements for hydrides.

Hydride	a [Å]	b [Å]	c [Å]
TiFe+H	2.9672(1)	4.5480(2)	4.4015(2)
$Ti_{0.9}Hf_{0.1}Fe_{0.9}Ni_{0.1}$+H	2.9684(2)	4.5570(3)	4.4096(2)
$Ti_{0.8}Hf_{0.2}Fe_{0.8}Ni_{0.2}$+H	2.8316(2)	4.5123(2)	4.4056(2)

TABLE IV

Chemical composition derived from EDS analysis.

Sample	[At. %]			
	Ti	Fe	Ni	Hf
TiFe	49.5(3)	50.5(2)		
$Ti_{0.8}Hf_{0.2}Fe$	27.5(3)	58.9(3)		13.6(2)
	45.1(2)	52.5(3)		2.4(2)
$Ti_{0.9}Hf_{0.1}Fe_{0.9}Ni_{0.1}$	31.5(3)	55.4(4)	1.4(2)	11.7(2)
	45.1(2)	46.1(3)	6.0(2)	2.7(2)
$Ti_{0.8}Hf_{0.2}Fe_{0.8}Ni_{0.2}$	26.9(2)	56.9(4)	3.7(2)	12.5(3)
	44.6(3)	41.5(3)	11.1(2)	2.8(2)

substituting Ni for Fe stabilizes the cubic structure of the $Ti_{1-x}Hf_xFe_{1-y}Ni_y$ alloys. It is an interesting observation, as for single Hf or Ni doping, disproportionation of the main cubic TiFe phase was observed [11–13].

According to Fig. 2, the main reflection is shifted toward a low angle, and additionally, the reflection shows splitting. It is established that $TiFeH_x$, where $x \approx 1$, changes the crystal structure from the cubic $Pm\text{-}3m$ (the α-phase) into the orthorhombic $P222_1$ one (the β-phase) [15]. For higher hydrogen concentrations ($x < 2$), the centered orthorhombic $Cmmm$ space group is adopted (the γ-phase) [16].

The obtained diffraction patterns of hydrides could be indexed by the $P222_1$ space group. This is consistent with the hydrogen concentrations, which are slightly higher than for the pure β-phase. The lattice parameters for the $TiFeH_1$ phase (β-phase) were reported to be $a = 2.956$ Å, $b = 4.543$ Å, and $c = 4.388$ Å [15]. Our results, listed in Table III, show consistently larger lattice parameters; however, the obtained hydrogen concentrations were somewhat higher.

It is extremely interesting that hydriding suppresses the occurrence of the spurious phases visible in the parent alloys, except for the TiFe. The strains derived from refinements are rather high and exceed 1%, which suggests that a significant amount of defects are raised by hydrogen introduction to the primary structures.

Scanning electron microscopy images show that the samples are solid without significant cracks. Imaging with backscattered electrons revealed the presence of two easily distinguishable phases for all the samples, excluding the parent TiFe one, which is chemically homogenous. As can be seen in Fig. 3,

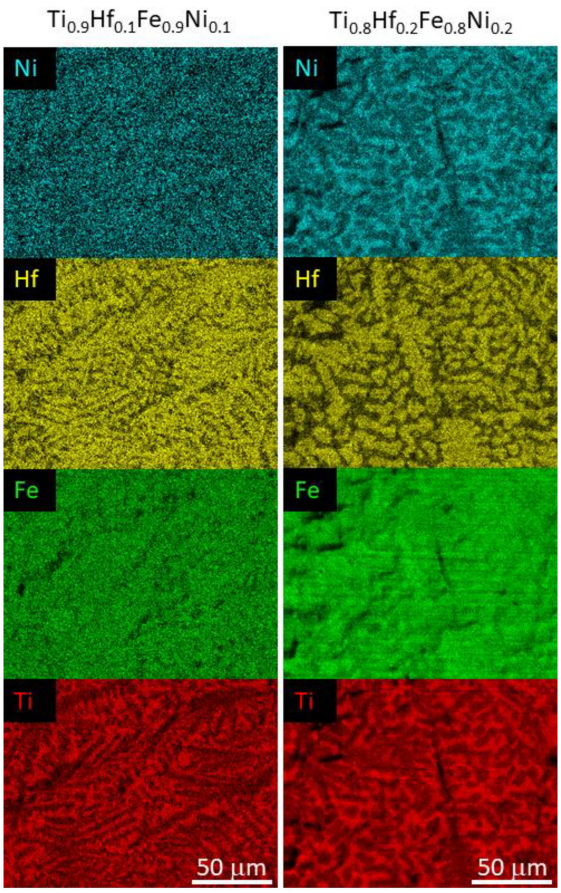

Fig. 3. Energy-dispersive X-ray spectroscopy (EDS) based maps of $Ti_{0.9}Hf_{0.1}Fe_{0.9}Ni_{0.1}$ and $Ti_{0.8}Hf_{0.2}Fe_{0.8}Ni_{0.2}$ samples.

the two phases differ in terms of Hf/Ni content (see also Table IV). In the case of the sample without Ni addition, an important excess of iron is clearly visible, suggesting either the formation of a non-stoichiometric TiFe or the presence of additional Fe in Hf-rich regions. For double-substituted (by Hf and Ni) samples, the Ti- or Hf-rich structures are much finer for a smaller doping ratio.

The ^{57}Fe Mössbauer spectroscopy results for studied systems are presented in Figs. 4 and 5. The corresponding data is listed in Table V. The parent TiFe alloy exhibits cubic symmetry at the Fe (1a) sites surrounded by 8 Ti atoms at the 1b sites. Consequently, the Mössbauer spectrum is a narrow single line with no quadrupole splitting (Δ) [17–19]. However, for the amorphous TiFe alloy, an additional component with Δ was involved [17].

In fact, spectra recorded for our as-cast TiFe alloy exhibit two components: one singlet (Fe1 without quadrupole splitting) and a doublet (Fe2). The doublet originates from the randomization of the iron environments as a result of atomic exchange between the 1b and 1a sites, as confirmed by X-ray diffraction. It results in non-symmetric Fe local environments, where one or more of the Ti ligands are

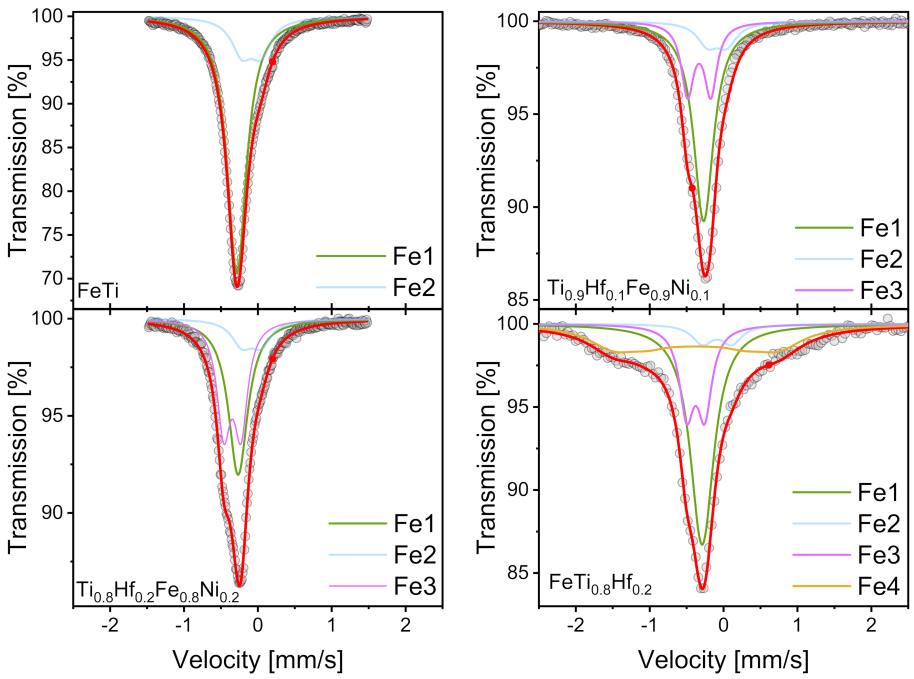

Fig. 4. Mössbauer spectroscopy results for studied alloys before hydrogenation. For parameters of the components labelled Fe1–Fe4, see Table V and text.

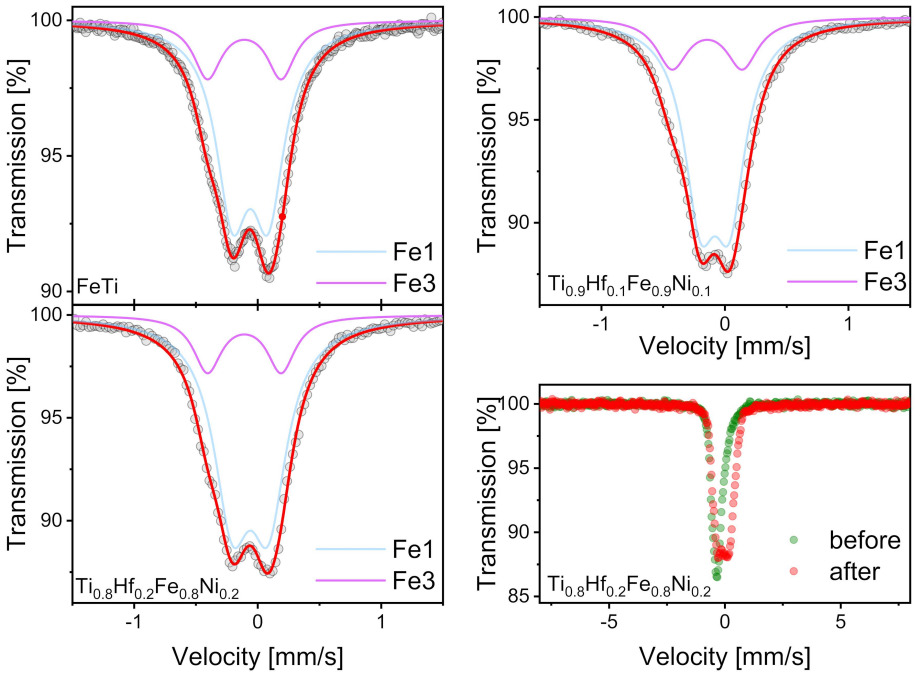

Fig. 5. Mössbauer spectroscopy results for $TiFeH_x$ hydrides. For parameters of the components labeled Fe1-Fe4, see Table V and text. The last panel shows 57Fe Mössbauer spectra for $Ti_{0.8}Hf_{0.2}Fe_{0.8}Ni_{0.2}$ before and after hydrogenation.

replaced by Fe. The share of the Fe2 component of about 17.3% is in agreement with the refinement of the XRD pattern of TiFe discussed above (assuming the same Lamb–Mössbauer factors for both components).

For $Ti_{0.9}Hf_{0.1}Fe_{0.9}Ni_{0.1}$ and $Ti_{0.8}Hf_{0.2}Fe_{0.8}Ni_{0.2}$, an additional Fe3 component appears. The component is most likely related to the statistical distribution of Hf and Ni atoms over the 1a and 1b sites, which, in the case of $Ti_{0.9}Hf_{0.1}Fe_{0.9}Ni_{0.1}$, produces

TABLE V

Results of Mössbauer spectroscopy studies: contribution to the spectra (Fe1–Fe4), isomer shift (δ), and quadrupole splitting (Δ).

	Contribution [%]	δ [mm/s]	Δ [mm/s]
TiFe			
Fe1	82.7(2)	−0.175(1)	–
Fe2	17.3(2)	0.020 (1)	0.256(6)
$Ti_{0.9}Hf_{0.1}Fe_{0.9}Ni_{0.1}$			
Fe1	61.7(3)	−0.161(1)	–
Fe2	12.3(4)	0.020(1)	0.256(6)
Fe3	26.0(3)	−0.221(1)	0.313(9)
$Ti_{0.8}Hf_{0.2}Fe_{0.8}Ni_{0.2}$			
Fe1	46.0(4)	−0.158(1)	–
Fe2	11.4(4)	0.020(1)	0.256(6)
Fe3	42.6(3)	−0.232(1)	0.242(1)
$Ti_{0.8}Hf_{0.2}Fe$			
Fe1	48.6(2)	−0.181(1)	–
Fe2	5.3(4)	0.020(1)	0.242(5)
Fe3	19.3(2)	−0.268(3)	0.394(1)
Fe4	26.8(4)	−0.263(3)	–
TiFe + H			
Fe1	79.1(2)	0.049(8)	0.269(1)
Fe3	20.9(2)	0.001(3)	0.556(1)
$Ti_{0.9}Hf_{0.1}Fe_{0.9}Ni_{0.1}$ + H			
Fe1	79.9(2)	0.027(1)	0.232(1)
Fe3	20.1(3)	−0.034(2)	0.568(5)
$Ti_{0.8}Hf_{0.2}Fe_{0.8}Ni_{0.2}$ + H			
Fe1	82.6(3)	0.049(1)	0.289(5)
Fe3	17.4(5)	0.001(1)	0.596(8)

larger electric field gradients compared to the Fe2 component, as the respective Δ is higher. The share of the Fe3 component increases consistently with an increase in Hf and Ni.

For $Ti_{0.8}Hf_{0.2}Fe$, which shows a complex X-ray diffraction pattern, an additional Fe4 component with hyperfine magnetic field $B = 6.93(7)$ T was required to properly describe the observed spectrum. Unambiguous determination of the corresponding phase is difficult, but as XRD patterns consisted of few unindexed broad lines and were in agreement with chemical analysis data, it seems that this contribution can be assigned to some non-stoichiometric C14 Laves phase(s) of presumably $(HfTi)(Fe)_2$ composition. The C14 $HfFe_2$ phase exhibits soft magnetic properties with a magnetic contribution to Mössbauer spectra at room temperature [20]. Yet, it seems that the main cubic Pm-$3m$ phase is still nonmagnetic, similar to other investigated alloys.

For $TiFeH_x$ hydrides, Mössbauer spectroscopy typically shows two components, depending on the hydrogen concentration (see Fig. 5). For significant amounts of absorbed hydrogen, the spectra typically consist of two or more components with isomer shifts (δ) close to zero or positive for $TiFeH_{1.7}$ [21]. For Ni-substituted TiFe alloys, Mössbauer spectroscopy results revealed a similar situation [22]. However, it must be taken into account that the hydrides were produced from annealed parent materials, and therefore, no substantial atomic disorder could be expected.

For our materials, the spectra can be modeled by 2 doublets (Fe1 and Fe3) with relatively small positive and negative δ. The main doublet Fe1 seems to have evolved from the single Fe1 line of the parent compound, and the corresponding δ raised substantially. According to self-consistent energy-band calculations for the TiFe alloy, the isomer shift originates from the density of conduction states (formed mainly by d states, but also s ones) [23]. Therefore, the observed nearly zero isomer shifts for hydrides are apparently related to a decrease in the conduction electron density resulting from the screening of H atoms incorporated into the crystal structure. Similarly to the parent alloys, the Fe3 contribution is probably the Hf-related feature with high Δ. The Fe3 component also exhibits a shift towards higher δ, for the same reason as discussed for the Fe1 one. Similar parameters refined for hydrides are consistent with XRD data, where resulting diffraction patterns were qualitatively similar.

For all specimens, spectra with higher velocity were also recorded in order to track magnetic precipitations originating from pure Fe or iron oxides. Samples of such spectra for raw $Ti_{0.8}Hf_{0.2}Fe_{0.8}Ni_{0.2}$ and its hydride are presented in Fig. 5.

4. Conclusions

In this work, we determined structural and microstructural properties, as well as hyperfine interactions, in double-substituted as-cast TiFe alloys for hydrogen storage. The results obtained for the compounds $Ti_{1-x}Hf_xFe_{1-y}Ni_y$ revealed that simultaneous substitution of Hf and Ni into the TiFe matrix leads to the stabilization of the cubic Pm-$3m$ structure, while only Hf substitution leads to severe sample disproportionation. The as-cast materials with segregated surface, as proved by XRD, electron microscopy, and Mössbauer spectroscopy, exhibit substantially better thermodynamic conditions for activation towards hydrogen absorption. Moreover, the proposed stoichiometry with a certain degree of atomic disorder introduced produces nearly single-phased hydrides with no typical impurities like Laves phases that hamper the hydrogen uptake at subsequent cycles. Hydrogen sorption measurements suggested that the $Ti_{0.9}Hf_{0.1}Fe_{0.9}Ni_{0.}1$ alloy exhibits properties that can be optimized for hydrogen storage systems.

Mössbauer spectroscopy was proven to be an excellent tool for the investigation of TiFe-related alloys and their hydrides. According to our results, the hydrogenation of the synthesized alloys leads to a significant decrease in the conducting electronic states in the compounds because of the necessity of screening of repulsive interactions between hydrogen (protons) occupying its sites in the crystal structure of the hydrides. Furthermore, the structural disorder introduced to facilitate the activation of the alloys could be precisely tracked by XRD and electron microscopy studies.

Acknowledgments

This work was partially supported (synthesis, X-ray diffraction, electron microscopy studies, data consolidation) by the National Science Centre, Poland, number: 2023/05/Y/ST3/00249 under the M-ERA.NET 3 Call 2023 (project acronym "HYPHAD", Horizon 2020 grant agreement No. 958174. Financial support by the National Science Centre, Poland, Grant No. 2021/41/B/ST3/03454 is acknowledged. The research project was partly supported by the program "Excellence Initiative — Research University" for the AGH University of Krakow.

References

[1] Y. Shang, S. Liu, Z. Liang et al., *Commun. Mater.* **3**, 101 (2022).

[2] Y.-H. Zhang, C. Li, Z.-M. Yuan, Y. Qi, S.-H. Guo, D.-L. Zhao, *J. Iron Steel Res. Int.* **29**, 537 (2022).

[3] M.V. Lototsky, M.W. Davids, V.N. Fokin, E.E. Fokina, B.P. Tarasov, *Therm. Eng.* **71**, 264 (2024).

[4] H. Liu, J. Zhang, P. Sun, C. Zhou, Y. Liu, Z.Z. Fang, *J. Energy Storage* **68**, 107772 (2023).

[5] L. Schlapbach, T. Riesterer, *Appl. Phys. A* **32**, 169 (1983).

[6] J.G. Li, X.J. Jiang, Z.N. Li, L.J. Jiang, X.G. Li, *Int. J. Energy Res.* **43**, 5759 (2019).

[7] L. Luo, Y.Z. Li, T.T. Zhai, F. Hu, Z.W. Zhao, X. Bian, W.Y. Wu, *Int. J. Hydrogen Energy* **44**, 25188 (2019).

[8] H.Y. Leng, Z.G. Yu, Q. Luo, J. Yin, N. Miao, Q. Li, K.C. Chou, *Int. J. Hydrogen Energy* **45**, 19553 (2020).

[9] K. Sakine, R. Mohammad, H. Jacques, *J. Alloy. Compd.* **775**, 912 (2019).

[10] H.W. Shang, Y.Q. Li, Y.H. Zhang, Y. Qi, S.H. Guo, D.L. Zhao, *Int. J. Hydrogen Energy* **43**, 19091 (2018).

[11] M. Polański, M. Kwiatkowska, I. Kunce, J. Bystrzycki, *Int. J. Hydrogen Energy* **38**, 12159 (2013).

[12] V. Razafindramanana, S. Gorsse, J. Huot, J. Bobet, *Energies* **12**, 3477 (2019).

[13] Y.Q. Li, H.W. Shang, Y.H. Zhang, P. Li, Y. Qi, D.L. Zhao, *Int. J. Hydrogen Energy* **44**, 4240 (2019).

[14] J. Rodriguez-Carvajal, *Physica B* **192**, 55 (1993).

[15] P. Thompson, A.A. Pick, F. Reidinger, L.M. Corliss, J.M Hasting, J.J. Reilly, *J. Phys. F* **8**, L75e80 (1978).

[16] P. Fischer P, J. Schefer, K. Yvon, L. Schlapbach, T. Riesterer, *J. Less-Common Met.* **129**, 39 (1987).

[17] C.L. Chien, S.H. Liou, *Phys. Rev. B* **31**, 8238 (1985).

[18] D. Khatamian, F.D. Manchester, *Surf. Scien.* **186**, 309 (1987).

[19] G.K. Wertheim, J.H. Wernick, *Acta Metal.* **15**, 297 (1967).

[20] J. Belosevic-Cavor, V. Koteski, N. Novakovic, G. Concas, F. Congiu, G. Spano, *Eur. Phys. J. B* **50**, 425 (2006).

[21] L.J. Swartzendruber, L.H. Bennet, R.E. Watson, *J. Phys. F Met. Phys.* **6**, L331 (1976).

[22] B.T. Abe, K. Tanaka, M. Shimotomai, M. Doyama, *Trans. Jpn. Inst. Met.* **28**, 861 (1987).

[23] D.A. Papaconstantopoulos, *Phys. Rev. B* **11**, 4801 (1975).